

Convergence of phase noise in DPSK transmission systems by novel phase noise averagers

Chia Chien Wei and Jason (Jyehong) Chen

Department of Photonics and Institute of Electro-Optical Engineering, National Chiao-Tung University,
1001 Ta Hsueh Rd., Hsin-Chu, Taiwan, 300
mgys0.eo91g@nctu.edu.tw, jchen@mail.nctu.edu.tw

Abstract: This investigation proposes a novel all-optical phase noise averager to reduce residual phase noise in the differential phase-shift keying (DPSK) transmission system with phase-preserving amplitude regenerators. The proposed phase noise averager is based on a phase-sensitive amplifier but does not require an extra phase-locking optical pump beam. It can increase the correlation between the phase noises of neighboring bits and greatly reduce the differential phase noise in the transmission system. Independently of the cascaded spans, analytical analysis demonstrates that, in the DPSK system with repeated averagers, the total differential phase noise will be less than that before the first averager. Theoretical analysis and numerical simulation are carried out and confirm the significant improvement of DPSK signals using the proposed novel phase noise averagers.

©2006 Optical Society of America

OCIS codes: (060.2330) Fiber optics communications; (060.2360) Fiber optics links and subsystems; (060.4370) Nonlinear optics, fibers; (060.5060) Phase modulation; (190.3270) Kerr effect; (190.4380) Nonlinear optics, four-wave mixing

References and links

1. A. Gnauck, "40-Gb/s RZ-differential phase shift keyed transmission," *Optical Fiber Communication Conference 2003*, paper ThE1.
2. J. K. Rhee, D. Chowdhury, K. S. Cheng, and U. Gliese, "DPSK 32×10 Gb/s transmission modeling on 5×90 km terrestrial system," *IEEE Photonics Technol. Lett.* **12**, 1627-1629 (2000).
3. A. H. Gnauck, X. Liu, X. Wei, D. M. Gill, and E. C. Burrows, "Comparison of modulation formats for 42.7-Gb/s single-channel transmission through 1980 km of SSMF," *IEEE Photonics Technol. Lett.* **16**, 909-911 (2004).
4. J. P. Gordon and L. F. Mollenauer, "Phase noise in photonic communication systems using linear amplifiers," *Opt. Lett.* **15**, 1351-1353 (1990).
5. C. J. McKinstrie, C. Xie, and C. Xu, "Effects of cross-phase modulation on phase jitter in soliton systems with constant dispersion," *Opt. Lett.* **28**, 604-606 (2003).
6. C. J. McKinstrie, S. Radic, and C. Xie, "Reduction of soliton phase jitter by in-line phase conjugation," *Opt. Lett.* **28**, 1519-1521 (2003).
7. S. L. Jansen, D. van den Borne, G. D. Khoe, H. de Waardt, C. C. Monsalve, S. Spalter and P. M. Krummrich, "Reduction of nonlinear phase noise by mid-link spectral inversion in a DPSK based transmission system," *Optical Fiber Communications 2005*, paper OTh05.
8. X. Liu, X. Wei, R. E. Slusher, and C. J. McKinstrie, "Improving transmission performance in differential phase-shift-keyed systems by use of lumped nonlinear phase-shift compensation," *Opt. Lett.* **27**, 1616-1618 (2002).
9. C. Xu and X. Liu, "Post-nonlinearity compensation with data-driven phase modulators in phase-shift keying transmission," *Opt. Lett.* **27**, 1619-1621 (2002).
10. S. A. Derevyanko and S. K. Turitsyn, "Reduction of the phase jitter in differential phase-shift-keying soliton transmission systems by in-line Butterworth filters," *Opt. Lett.* **29**, 35-37 (2004).

11. D. Boivin, M. Hanna, P.-A. Lacourt, and J.-P. Goedgebuuer, "Reduction of phase jitter in dispersion-managed systems by in-line filtering," *Opt. Lett.* **29**, 688-690 (2004).
12. P. V. Mamyshev, "All-optical data regeneration based on self-phase modulation effect," *European Conference on Optical Communication 1998*, pp. 475-476.
13. E. Ciaramella and S. Trillo, "All-optical signal reshaping via four-wave mixing in optical fibers," *IEEE Photon. Technol. Lett.* **12**, 849-851 (2000).
14. S. Mazumder and S. Yamashita, "Optical 2R regeneration of 10Gbps signal using cascaded fiber four wave mixing," *European Conference on Optical Communication 2005*, pp. 57-58.
15. K. Croussore, C. Kim, and G. Li, "All-optical regeneration of differential phase-shift keying signals based on phase-sensitive amplification," *Opt. Lett.* **29**, 2357-2359 (2004).
16. K. Croussore, I. Kim, C. Kim, Y. Han, and G. Li, "Phase-and-amplitude regeneration of differential phase-shift keyed signals using a phase-sensitive amplifier," *Opt. Express* **14**, 2085-2094 (2006).
17. M. Shin, P. S. Devgan, V. S. Grigoryan, and P. Kumar, "SNR improvement of DPSK signals in a semiconductor optical regenerative amplifier," *IEEE Photonics Technol. Lett.* **18**, 49-51 (2006).
18. A. Striegler and B. Schmauss, "All-optical DPSK signal regeneration based on cross-phase modulation," *IEEE Photonics Technol. Lett.* **16**, 1083-1085 (2004).
19. A. G. Striegler, M. Meissner, K. Cvecek, K. Sponsel, G. Leuchs, and B. Schmauss, "NOLM-based RZ-DPSK signal regeneration," *IEEE Photonics Technol. Lett.* **17**, 639-641 (2005).
20. M. Matsumoto, "Regeneration of RZ-DPSK signals by fiber-based all-optical regenerators," *IEEE Photonics Technol. Lett.* **17**, 1055-1057 (2005).
21. S. Boscolo, R. Bhamber, and S. K. Turitsyn, "Design of Raman-based NOLM for optical 2R regeneration of RZ-DPSK transmission," *Optical Fiber Communication Conference 2006*, paper OWJ5.
22. K.-P. Ho, "Asymptotic probability density of nonlinear phase noise," *Opt. Lett.* **28**, 1350-1352 (2003).
23. A. Mecozzi, "Probability density functions of the nonlinear phase noise," *Opt. Lett.* **29**, 673-675 (2004).
24. C. Xu, X. Liu, and X. Wei, "Differential phase-shift keying for high spectral efficiency optical transmissions," *IEEE J. Sel. Top. Quantum Electron.* **10**, 281-293 (2004).
25. X. Zhang, Z. Qu, and G. Yang, "Probability density function of noise statistics for optically pre-amplified DPSK receivers with optical Mach-Zehnder interferometer demodulation," *Opt. Commun.* **258**, 177-183 (2006).
26. X. Wei and X. Liu, "Analysis of intrachannel four-wave mixing in differential phase-shift keying transmission with large dispersion," *Opt. Lett.* **28**, 2300-2302 (2003).
27. L. K. Wickham, R.-J. Essiambre, A. H. Gnauck, P. J. Winzer, and A. R. Chraplyvy, "Bit pattern length dependence of intrachannel nonlinearities in pseudolinear transmission," *IEEE Photonics Technol. Lett.* **16**, 1591-1593 (2004).

1. Introduction

In differential phase-shift keying (DPSK) format, an optical pulse appears in each bit slot with the binary data encoded as either a zero or π phase shift between adjacent bits. This format emerged as an alternative to the on-off keying (OOK) format, especially for long-haul transmission [1]. The most obvious advantage of the DPSK format with balanced detection over OOK is that its optical signal-to-noise ratio (OSNR) required to reach a given bit-error ratio (BER) is approximately 3 dB lower [1]. DPSK signals are also less sensitive to nonlinear effects, particularly those of inter-channel cross-phase modulation (XPM) [2], improved dispersion tolerance and high spectral efficiency [3]. Without considering timing jitter, unlike OOK systems that are limited only by amplitude noise (AN), DPSK systems are restricted by both AN and phase noise (PN). The PN in DPSK systems will be converted to AN in the receiver using a delay interferometer (DI). Furthermore, the PN contains linear PN and nonlinear PN. In dispersion-managed systems, AN and linear PN are generated mainly from the amplified spontaneous emission (ASE) noise of optical amplifiers. The nonlinear PN is translated from AN through the fiber Kerr effect, often called the Gordon-Mollenauer effect [4], and dispersion-induced pattern effects through XPM in wavelength-division multiplexed (WDM) systems [5].

Either PN or AN must be prevented from being accumulated to expand the reach of DPSK systems. Spectral inversion by phase conjugation [6, 7] and post nonlinear phase-shift compensators [8, 9] has been proposed to reduce accumulated nonlinear PN. However, these approaches are rather difficult to realize. Although in-line filtering is a simple means of

constraining PN by the stabilization of amplitude [10, 11], in-line regenerators for DPSK signals are needed to manage either AN or PN and to further expand the transmission distance. Unfortunately, most of the all-optical regeneration schemes for OOK format [12-14] do not fit the DPSK format because the phase information is distorted by these regenerators. Theoretically, a phase-sensitive amplifier (PSA) can simultaneously reduce both AN and PN, and the regeneration was experimentally demonstrated by pumping a PSA with an original undistorted DPSK signal [15, 16]. Even so, the coherent pump beam in a PSA is difficult to realize in the real world, owing to optical-carrier phase-locking between the pump beam and the signal beam. Recently, a nonlinear optical loop mirror (NOLM) with a semiconductor optical amplifier (SOA) [17] has been found to yield slight SNR improvements in DPSK signals, but not to be effective in extending the reach of DPSK systems. Additionally, several phase-preserving amplitude regeneration approaches for DPSK format have been proposed [18-21]. The reduction of AN is such that the nonlinear PN caused by the Gordon-Mollenauer effect will be reduced [20, 21] and the transmission distance will be extended. Nevertheless, these regenerators can constrain only some of the nonlinear PN and preserve the original linear PN. They will also cause an additional PN that is transformed from AN. Therefore, the accumulated PN distorts DPSK signals and limits the transmission distance.

This work proposes a novel all-optical phase noise averager (PNA) that is based on a PSA. The proposed PNA can average the PN of one bit with that of its neighboring bit coherently and does not need an extra phase-locking pump beam. These PNAs can effectively diminish differential PN and greatly extend the reach of DPSK signals. The most important and appealing feature of the proposed PNA is that, when cascaded, the chain of PNAs results in the convergence of PN. In amplitude-managed DPSK systems with repeated PNAs, the total differential PN is always less than that before the first averager and is irrelevant to the number of DPSK spans.

2. Concept and capability of a PNA

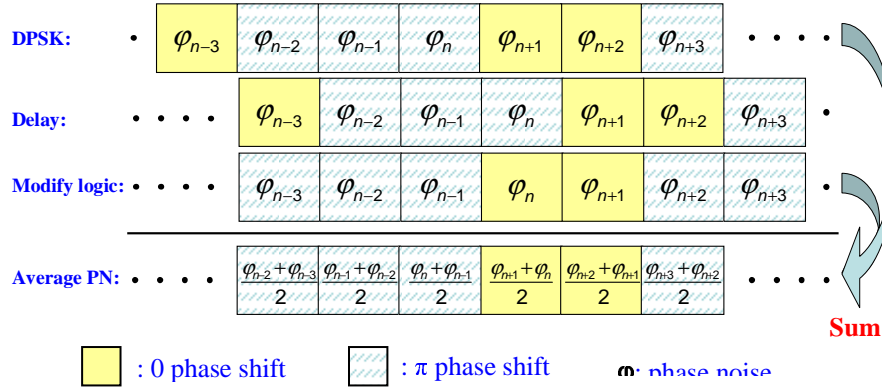


Fig. 1. Concept of a PNA

The function of a PNA is to average the PN of one bit with that of its adjacent bit. Figure 1 presents a simple concept in the realization of a PNA. Based on an assumption that signals all have a constant amplitude, E_0 , each bit of the DPSK signals can be represented as, $E_n = s_n \cdot E_0 \exp(j\varphi_n)$, where $s_n = \pm 1$ corresponds to a zero or π phase shift and φ_n is random PN. After one bit delay, if the logic of the delay data sequence can be modified to be equivalent to that of the original DPSK data, as shown in Fig. 1, then the sum of this modified signals and the original signals can be written as,

$$E_{n,avg} = 2s_n E_0 \cos\left(\frac{\varphi_n - \varphi_{n-1}}{2}\right) \times e^{j\frac{\varphi_n + \varphi_{n-1}}{2}} \quad (1)$$

Therefore, the output field will have original information and contain averaged PN and minor AN converted from the differential PN. Although nonlinear PN has stochastic properties dissimilar to Gaussian noise [22], it has been shown that combined linear and nonlinear PN almost follows Gaussian distribution [23]. Consequently, φ_n and φ_{n-1} can be treated as independent Gaussian noise with the same variance, σ^2 , without making significant errors. From Eq. (1), the variance of the output PN, $(\varphi_n + \varphi_{n-1})/2$, is $\sigma^2/2$. However, after demodulation via a DI, the received signals are influenced by the differential PN, $\Delta\varphi_n = \varphi_n - \varphi_{n-1}$, not by the PN itself [24, 25]. Namely, the variance of the original differential PN is $2\sigma^2$, and the differential PN becomes $(\varphi_n - \varphi_{n-2})/2$ with a variance of $\sigma^2/2$ after this PNA is applied. Accordingly, the PNA can increase the correlation between the PN of neighboring bits and reduce the differential PN.

Hence, when the original DPSK signals pass an ideal PNA for the first time, the variances of PN and differential PN become one half and one quarter, respectively. However, for cascaded PNAs, the correlation between the PN of neighboring bits is such that the PN variances do not decrease exponentially. If DPSK signals go through ideal PNAs M times, PN and differential PN can be represented as (Appendix A),

$$\varphi_n^{(M)} = \frac{\sum_{k=0}^M (C_k^M \cdot \varphi_{n-k})}{2^M} \quad (2)$$

$$\Delta\varphi_n^{(M)} = \varphi_n^{(M)} - \varphi_{n-1}^{(M)} = \frac{\varphi_n + \sum_{k=1}^M [(C_k^M - C_{k-1}^M) \cdot \varphi_{n-k}] - \varphi_{n-M-1}}{2^M} \quad (3)$$

where C_k^n is the binomial coefficient. Therefore, the variance of the differential PN is changed from $2\sigma^2$ to,

$$\langle (\Delta\varphi_n^{(M)})^2 \rangle = \frac{2 + \sum_{k=1}^M (C_k^M - C_{k-1}^M)^2}{2^{2M}} \times \sigma^2 \quad (4)$$

Considering the transmission system displayed in Fig. 2, a phase-preserving amplitude regenerator and a PNA are arranged following the transmission of K spans, which consist of standard single mode fibers (SSMFs), dispersion compensating fibers (DCFs) and EDFAs. Every K spans, random PN with a variance of σ^2 is generated. In this case, the final differential PN, $\Delta\Phi$, has a variance of,

$$\langle \Delta\Phi^2 \rangle = \sum_{N=1}^M \langle (\Delta\varphi_n^{(N)})^2 \rangle = \sum_{N=1}^M \left(\frac{2 + \sum_{k=1}^N (C_k^N - C_{k-1}^N)^2}{2^{2N}} \right) \times \sigma^2 \quad (5)$$

One of the most crucial and attractive features of the proposed PNA is that even after an ultra-long transmission distance, i.e. $M \rightarrow \infty$, the variance in Eq. (5) converges to $2\sigma^2$ (as derived in Appendix B), which equals to the variance of the differential PN before the first PNA. Comparatively, the variance of differential PN without PNAs is $2M\sigma^2$ after transmission. Based on Eq. (4) and Eq. (5), Fig. 3 illustrates differential PN variances with and without PNAs. Figure 3 clearly shows that the equivalent accumulated PN never exceeds

that generated in every K spans. It guarantees that the accumulated PN will not limit the reach of a DPSK transmission system with amplitude regenerators and PNAs.

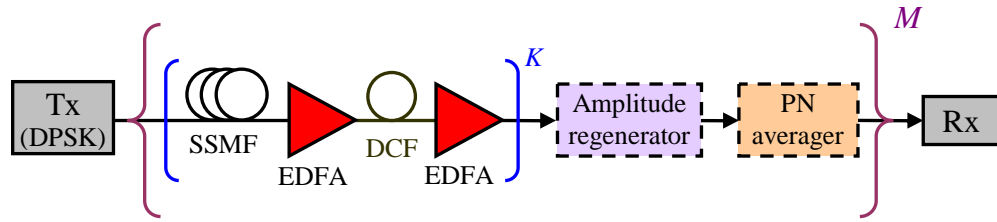


Fig. 2. Optical DPSK transmission system with amplitude regenerators and PNAs inserted every K spans.

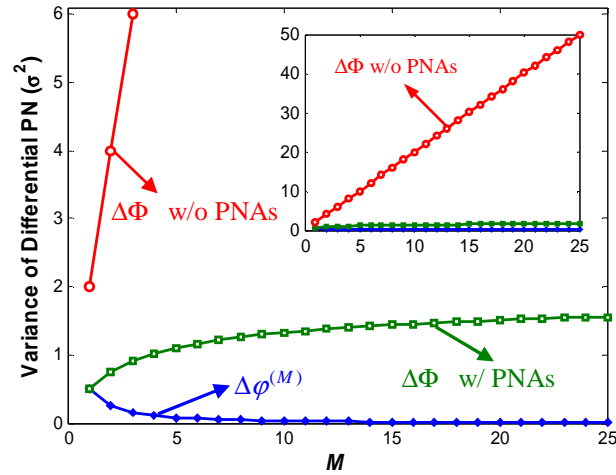


Fig. 3. The variances of differential PN as functions of the number of PNAs.

3. Realization and setup of a PNA

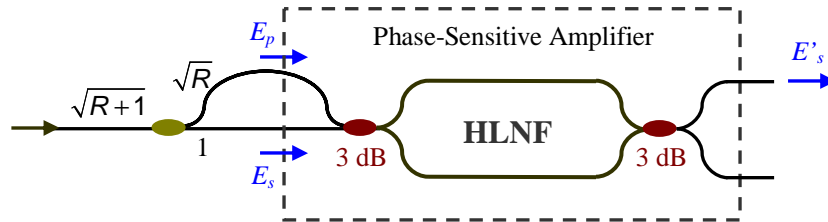


Fig. 4. Setup of a PNA

Figure 4 shows the setup of a PNA, which is made up by a PSA. With a pump beam, E_p , and a signal beam, E_s , the output field of a PSA is [15, 16],

$$E'_s = e^{j\theta_0} (E_s \cos \theta_{nl} - E_p \sin \theta_{nl}) \quad (6)$$

where $\theta_0 = (j\alpha L + \pi)/2 + \gamma L_{eff} (|E_s|^2 + |E_p|^2)/2$ and $\theta_{nl} = \gamma L_{eff} |E_s| |E_p| \sin(\phi_s - \phi_p)$. γ is the nonlinear coefficient of the highly nonlinear fiber (HNLN); α denotes the fiber loss; L is the fiber length; L_{eff} is the effective fiber length, and ϕ_s and ϕ_p are the signal and

pump phases, respectively. Equation (6) clearly reveals that the weighting term of E_p can modify its logic information to be identical with the data of the signal beam. The main difference between the proposed PNA and the conventional PSA is that a challenging phase-locking pump beam is not needed. The pump beam is replaced by the original signal beam with one bit delay and the power ratio of the pump beam to the signal beam is R , as shown in Fig. 4. Moreover, when this PNA is put after an ideal phase-preserving amplitude regenerator and the pump beam can be represent as $E_p = s_{n-1}E_0\sqrt{R}\exp(j\varphi_{n-1})$, the output filed becomes to $E'_s = e^{j\theta_0} \left(e^{j\Delta\varphi_n} - \Gamma_n\sqrt{R}\tan\vartheta_{nl} \right) \times s_n E_0 \cos\vartheta_{nl} e^{j\varphi_{n-1}}$, where $\Gamma_n = s_{n-1}/s_n = \pm 1$. Hence, Γ_n represents that the signal beam and pump beam are in-phase or out-phase. That is, $\sin(\phi_s - \phi_p)$ can be written as $\Gamma_n \times \sin(\Delta\varphi_n)$. As a result, Eq. (6) becomes,

$$E'_s = e^{j\theta_0} \left(e^{j\Delta\varphi_n} - \sqrt{R}\tan\vartheta_{nl} \right) \times s_n E_0 \cos\vartheta_{nl} e^{j\varphi_{n-1}} \quad (7)$$

where $\vartheta_{nl} = \Theta\sqrt{R}\sin(\Delta\varphi_n)$ and $\Theta = \gamma L_{eff} |E_s|^2$. Considering first-order approximation of trigonometric functions in Eq. (7), the bracket in Eq. (7) is the only part that is related to the differential PN and can be rewritten as,

$$\tilde{E}'_s = e^{j\Delta\varphi_n} - \Theta R \sin(\Delta\varphi_n) \quad (8)$$

The operating points can be derived from two conditions to yield the desired function of a PNA:

$$\frac{\partial(\angle\tilde{E}'_s)}{\partial\Delta\varphi_n} = \frac{1}{2} \quad \& \quad \frac{\partial|\tilde{E}'_s|^2}{\partial\Delta\varphi_n} = 0 \quad (9)$$

The first part of Eq. (9) guarantees that the PSA can average the PN and the second part minimizes the output AN induced by differential PN. Hence, from Eqs. (8) and (9), the operating points are $\Theta R = 1/\sqrt{2}$ and $\Delta\varphi_n = \Delta\varphi_Q = -\tan^{-1}(\sqrt{2})$. Setting $R = 10$ dB and $\Theta = 0.071$, Figs. 5(a)-5(c) presents the normalized output power, output phase and output phase slope of a PNA.

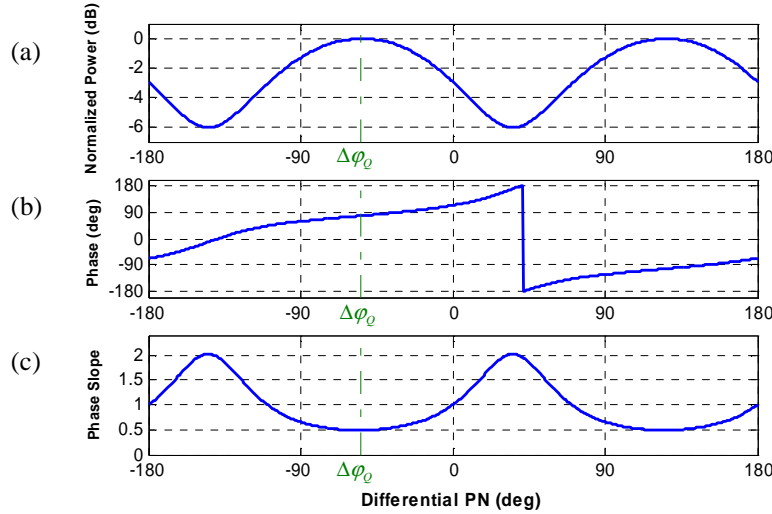


Fig. 5. (a). Normalized output power, (b) output phase and (c) output phase slope of a PNA.

phase slope of this PSA-based PNA, respectively. Therefore, when the splitting ratio of the first coupler in Fig. 4 is selected and a fixed phase difference $\Delta\varphi_0$ between the signal arm and the pump arm is given, a PSA can function as a PNA.

4. Simulation of RZ-DPSK transmission

The convergence of Eq. (5) is derived with an assumption of independent Gaussian PN. However, the assumption is not exactly true, especially for high data rate signals, such as 40 Gbps. This is because, at such data rate, intrachannel nonlinear effects, including intrachannel XPM (IXPM) and intrachannel four-wave mixing (IFWM) [26], have a greater impact on system performance, and IFWM introduces partially correlated PN on neighboring bits. In order to examine the effect of PNAs illustrated in Fig. 4 with actual PN, a single-channel 40 Gbps RZ-DPSK transmission system is then investigated.

The transmission system in our simulation is identical to the setup displayed in Fig. 2. The laser linewidth of the transmitter is 10 MHz and the duty cycle of RZ-DPSK is 33%. The length, dispersion, dispersion slope, nonlinear coefficient and loss of the SSMF are 80 km, 17 ps/nm/km, 0.07 ps/nm²/km, 1.3/W/km and 0.2 dB/km, respectively. For DCF, the corresponding parameters are 13.6 km, -100 ps/nm/km, -0.41 ps/nm²/km, 5.4/W/km and 0.65 dB/km. The noise figure (NF) of the EDFAs is 5 dB; the launch power into SSMFs and DCFs are 3 dBm and -3 dBm, respectively. The approach of the phase-preserving amplitude regenerator adopted in the simulation is based on the FWM effect in fibers because it has a simple structure. The characteristics of the FWM-based regenerator are described elsewhere [20], and in this regenerator, HNLF length, dispersion, dispersion slope, nonlinear coefficient, loss, $\Delta\lambda$ (wavelength difference between a pump beam and a DPSK signal beam), pump power, output peak power, and filter bandwidth are 1.5 km, 0.09 ps/nm/km, 0.03 ps/nm²/km, 16.2/W/km, 0.5 dB/km, 3 nm, 30 mW, 8.4 mW, and 160 GHz, respectively. The characteristics of the PNA in the simulation are described in Fig. 5. The transmitted signal is a De Bruijn sequence of 4096 bits, which provides sufficient pattern length to capture the interchannel nonlinear effects [27]. A FWM-based amplitude regenerator and a PSA-based PNA are inserted every 400 km of transmission, i.e. $K = 5$. Figure 6(a) displays the standard deviation (STD) of intensity noise (IN) normalized to the average peak power every 80 km of transmission. Figure 6(b) shows the STD of differential PN of DPSK signals at the corresponding distances. In the DPSK transmission system without regenerators and PNAs, normalized IN and differential PN increase absolutely with the transmission distance. With amplitude regenerators, IN can be effectively managed, but PN is still continuously accumulated. The PN initially declines at first and second regenerators due to the optical filter in the regenerators [10, 21]. However, the differential PN with regenerators exceeds that without regenerators after 1600 km, because the regenerators add extra PN [20]. If PNAs are inserted after regenerators, then the differential PN behind the averagers is constrained below that just in front of the first averager. Moreover, accumulation of differential PN in Fig. 6(b) is slightly faster than the analytical results depicted in Fig. 3, since the partially correlated PN of neighboring bits are considered in the simulation. Figures 7(a)-7(d) illustrate the differential phase constellations and differential phase eye-diagrams [24] of DPSK signals after 2800 km of transmission with and without PNAs. In Figs. 7(a) and 7(c), the DPSK signals without PNAs suffer from serious PN and the differential phase eye is almost closed. Consequently, although the amplitude of DPSK signals is managed well, as shown in Fig. 7(a), the groups with zero and π phase shifts almost overlap each other. When PNAs are used, PN is managed efficiently even after 2800 km of transmission and the performance of signals is effectively maintained.

Furthermore, in WDM systems, nonlinear PN induced by interchannel XPM effect has been shown to be strongly correlated between neighboring bits [5], as well as that induced by IFWM. When this kind of nonlinear PN dominate the whole PN, Eq. (4) should be modified

to consider the correlation between adjacent bits, and the effects of PNAs need to be re-examined.

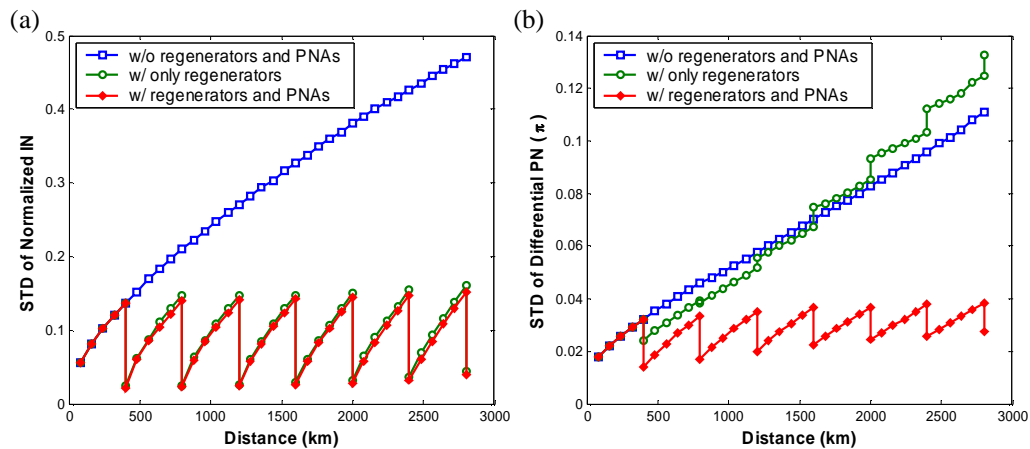


Fig. 6. (a). Normalized IN and (b) differential PN versus transmission distance for 40 Gbps 33% RZ-DPSK

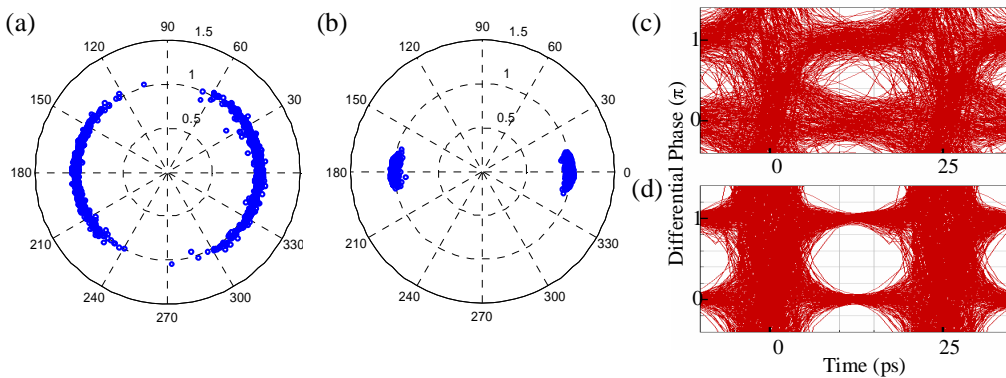


Fig. 7. Differential phasor diagrams for 40 Gbps 33% RZ-DPSK after 2800 km transmission. For (a), FWM-based regenerators are inserted, and for (b), FWM-based regenerators and PSA-based PNA are both inserted every 400 km. (c) and (d) are the differential phase eye-diagrams corresponding to (a) and (b), respectively.

5. Conclusion

This study proposes a novel all-optical PSA-based PNA that does not require a complicated optical coherent pump beam with optical phase-locking. The PNA can increase the correlation between PN of neighboring bits. Both theoretical analysis and numerical simulation confirm that inserting PNAs after in-line amplitude regenerators can effectively reduce the differential PN. The most significant and attractive feature of the proposed PNA is its ability to converge the cascaded PN. Additionally, the total differential PN is limited to less than that before the first averager and is independent of the number of DPSK spans. Accordingly, adding PNAs considerably improve the reach and performance of DPSK signals.

Appendix A

By considering the identity of binomial coefficients,

$$C_k^{n+1} = C_k^n + C_{k-1}^n \quad (\text{A.1})$$

and rewriting PN in Eq. (1) as $\phi'_n = (C_0^1 \cdot \phi_n + C_1^1 \cdot \phi_{n-1})/2$, the PN passing through PNA twice becomes,

$$\begin{aligned}\phi_n^{(2)} &= \frac{1}{2} \left(\frac{(C_0^1 \cdot \phi_n + C_1^1 \cdot \phi_{n-1})}{2} + \frac{(C_0^1 \cdot \phi_{n-1} + C_1^1 \cdot \phi_{n-2})}{2} \right) \\ &= \frac{C_0^2 \cdot \phi_n + C_1^2 \cdot \phi_{n-1} + C_2^2 \cdot \phi_{n-2}}{2^2}\end{aligned}\quad (\text{A.2})$$

With the same processing and expanding $\phi_n^{(M)}$, the coefficient of ϕ_{n-k} is C_k^M . Accordingly, $\phi_n^{(M)}$ can be represented as Eq. (2).

Appendix B

Express the sum of square of differential binomial coefficients as,

$$\sum_{k=1}^n (C_k^n - C_{k-1}^n)^2 = 2 \times \sum_{k=1}^n (C_k^n)^2 + 2 \times \sum_{k=1}^n (C_{k-1}^n)^2 - \sum_{k=1}^n (C_k^n + C_{k-1}^n)^2 \quad (\text{B.1})$$

Also, the binomial coefficients satisfy the identity,

$$\sum_{k=0}^n (C_k^n)^2 = C_n^{2n} \quad (\text{B.2})$$

where C_n^{2n} represents the central binomial coefficient. Using the identities of Eqs. (A.1) and (B.2), Eq. (B.1) can be modified as,

$$\begin{aligned}\sum_{k=1}^n (C_k^n - C_{k-1}^n)^2 &= 2 \times (C_n^{2n} - C_0^n) + 2 \times (C_n^{2n} - C_n^n) - (C_{n+1}^{2n+2} - C_0^{n+1} - C_{n+1}^{n+1}) \\ &= 4 \times C_n^{2n} - C_{n+1}^{2n+2} - 2 = \frac{2}{n+1} C_n^{2n} - 2\end{aligned}\quad (\text{B.3})$$

Due to a scaled form of the central binomial coefficient known as a Catalan number,

$$\mathbb{C}_n = \frac{C_n^{2n}}{n+1} \quad (\text{B.4})$$

the coefficient of Eq. (5) becomes,

$$\sum_{N=1}^M \left[\frac{2 + \sum_{k=1}^N (C_k^N - C_{k-1}^N)^2}{2^{2N}} \right] = 2 \times \sum_{N=1}^M \left(\frac{\mathbb{C}_N}{2^{2N}} \right) \quad (\text{B.5})$$

Additionally, these Catalan numbers have the generating function,

$$\frac{1 - \sqrt{1 - 4x}}{2x} = \sum_{n=0}^{\infty} (\mathbb{C}_n \cdot x^n) = 1 + x + 2x^2 + 5x^3 + \dots \quad (\text{B.6})$$

Therefore, as M in Eq. (B.5) approaches infinite, the summation converges,

$$\lim_{M \rightarrow \infty} 2 \times \sum_{N=1}^M \left[\mathbb{C}_N \cdot \left(\frac{1}{4} \right)^N \right] = 2 \quad (\text{B.7})$$

Acknowledgment

The authors would like to thank the National Science Council, Republic of China, Taiwan for financially supporting this research under Contract No. NSC 93-2215-E-009-027, NSC-95-2752-009-004